Supporting Information

Photoluminescence and magnetism integrated multifunctional black phosphorus probes through controllable P=O bonds orbital hybridization

S. Y. Wu[a], R. L. Qian[a], C. L. Ma*[a], Y. Shan*[b], Y. J. Wu[c], X. Y. Wu*[d], J. L. Zhang[a], X. B. Zhu[e], H.T. Ji[a], C. Y. Qu[a], F. Hou[a] and L. Z. Liu[f]

[a]Jiangsu Key Laboratory of Micro and Nano Heat Fluid Flow Technology and Energy Application, School of Physical Science and Technology, Suzhou University of Science and Technology, Suzhou, 215009, China

[b] Key Laboratory of Advanced Functional Materials of Nanjing, Nanjing Xiaozhuang University, Nanjing 211171, China

[c]Department of Neurology, Suzhou Science and Technology Town Hospital affiliated to Nanjing Medical University, Suzhou, 215009, China

[d]School of Traditional Chinese Medicine, Capital Medical University, Beijing, 100069, China

[e]School of Mechano-Electronic Engineering, Suzhou Vocational University, Suzhou, Jiangsu 215104, China

[f] National Laboratory of Solid State Microstructures and School of Physics, Nanjing University, Nanjing 210093, China
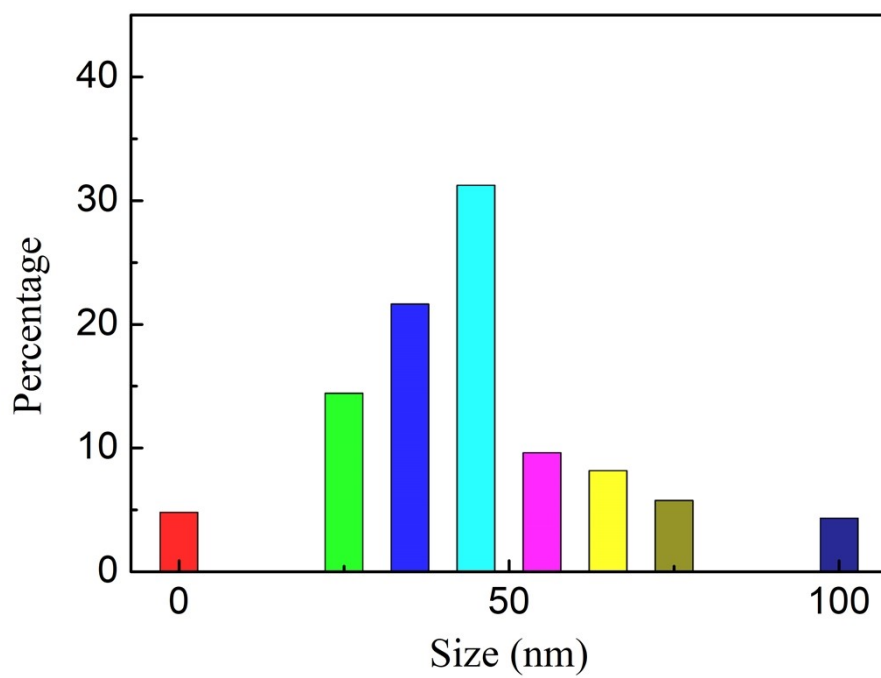
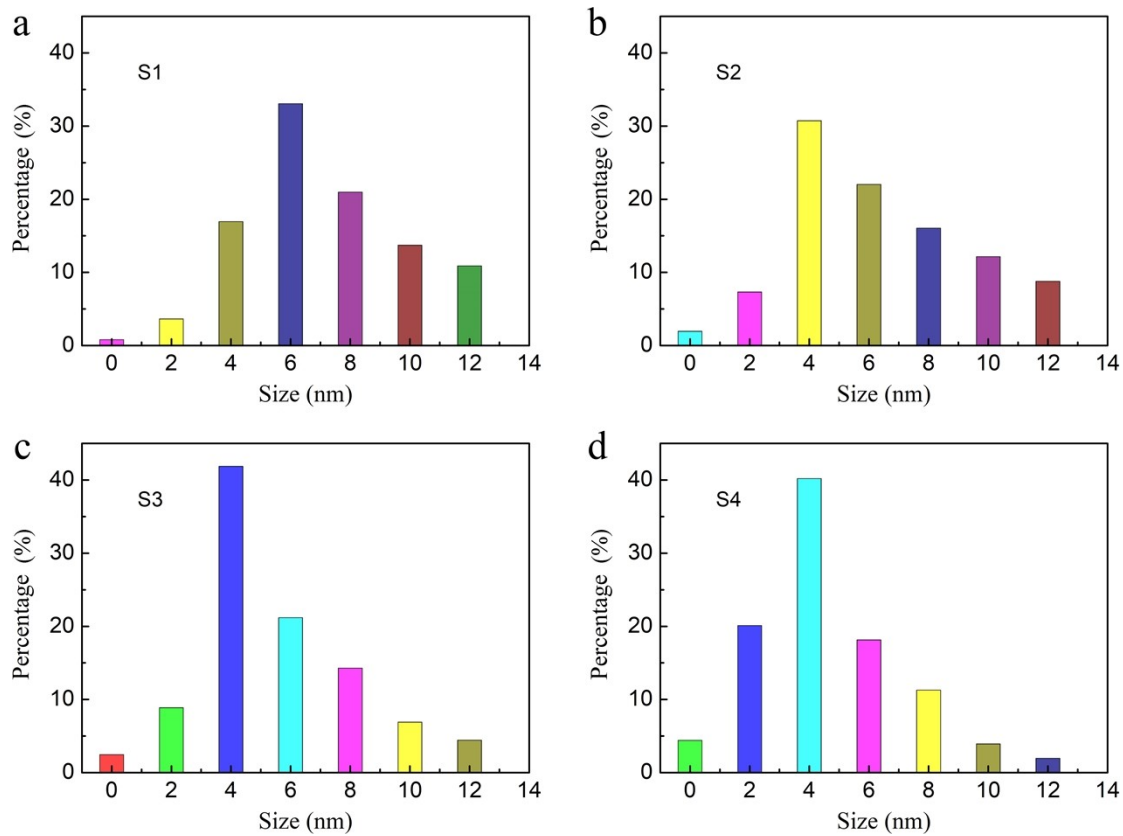Fig. S1. Size distribution of the passivated BP nanosheets (total number = 300).

Fig. S2. Size distribution of the isolated BP domains from S1 (a), S2 (b), S3 (c) and S4 (d) (total
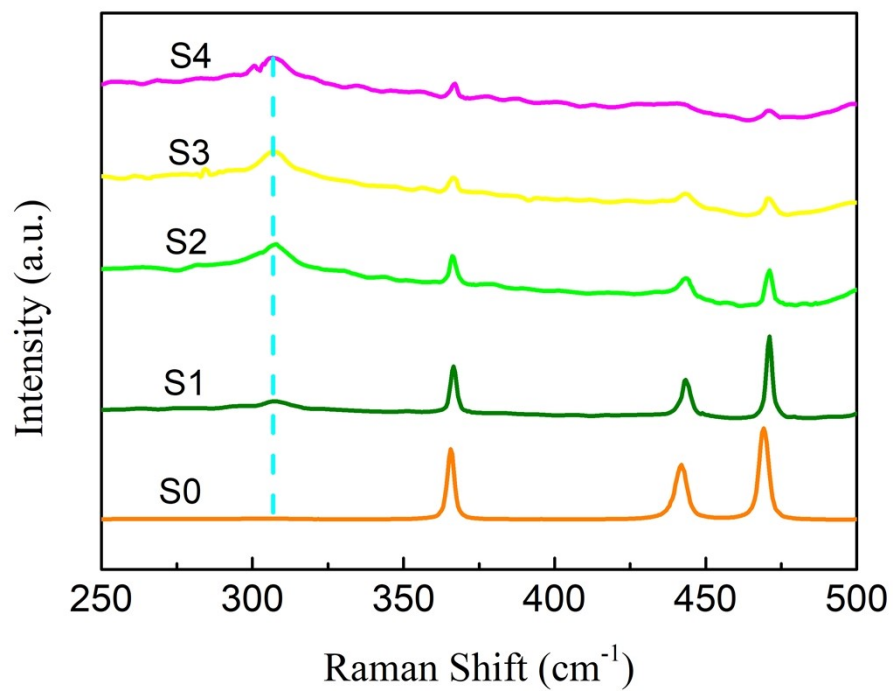
number = 300 for every sample).

Fig. S3. Measured Raman spectra from the BP nanosheets for different oxidation time. The P=O bonds relative Raman mode (marked by dashed lines) are enhanced as oxidation time.
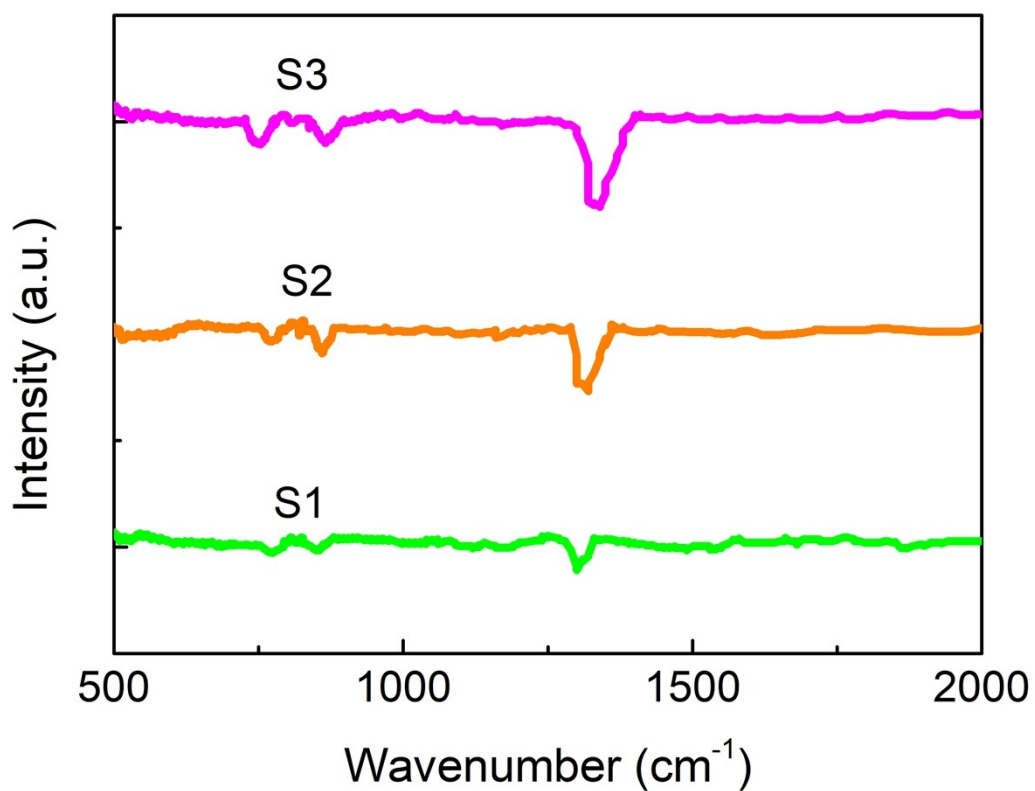
Fig. S4. FTIR spectra from the BP nanosheets for different oxidation time. The absorption peak at around 1315 cm^{-1} can be attributed to P=O groups, and the peaks at about 850 cm^{-1} and 770 cm^{-1} can be assigned to symmetric P−O−P vibrations and asymmetric P−O−P stretches, respectively (see, Langmuir, 2019, 35, 2172−2178).
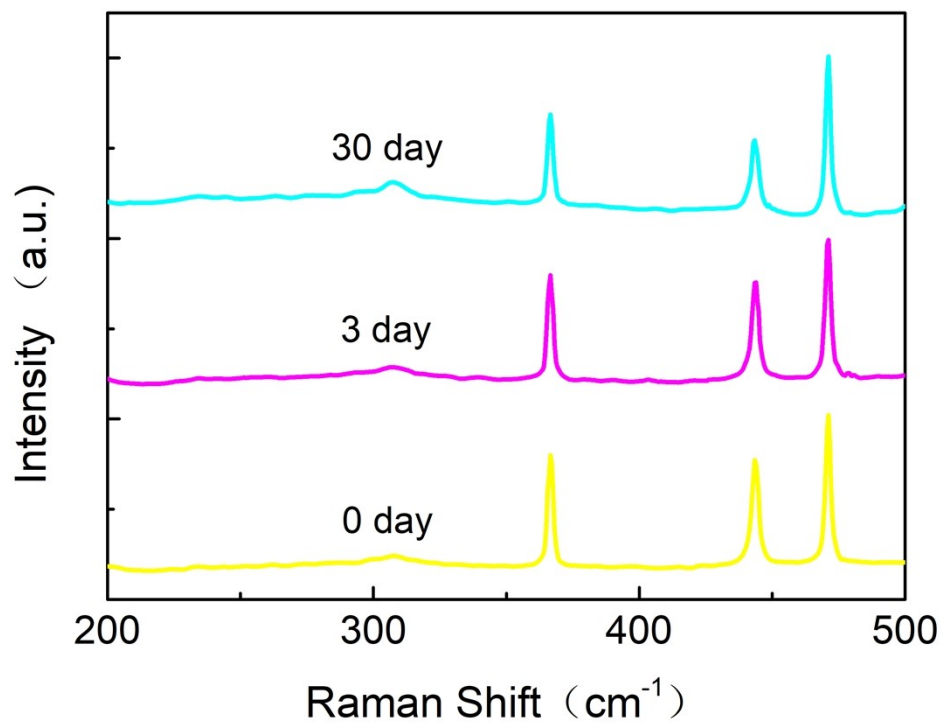
Fig. S5. Raman spectra of nanosheets with different treatment time under ambient condition.
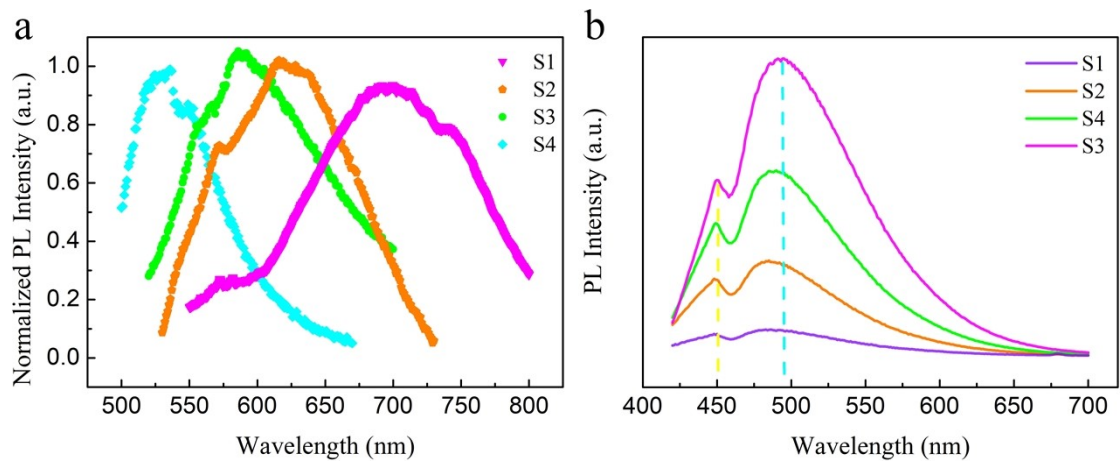
Fig. S6. PL spectra of the BP nanosheets for different oxidation time with a fixed excitation

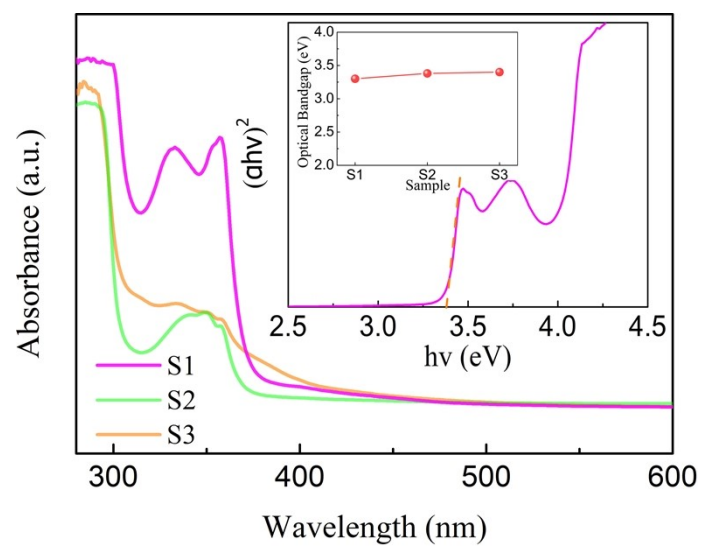wavelength of 532nm (a) and 400 nm (b).

Fig. S7. UV-Visible spectra of the BP nanosheets. Inset: Tauc plot curves of the nanosheets related to the optical bandgaps.

Table 1. Single exponential fitting of the PL decay curves monitored at 450nm and 480nm for different samples.

Sample τ (ns)	Sample1	Sample 2	Sample 3	Sample 4
τ_{450}	1.78	1.47	1.24	1.16
τ_{480}	1.35	1.29	1.15	1.02

Table 2. Bi-exponential fitting of the PL decay curves monitored at 580nm for different samples.

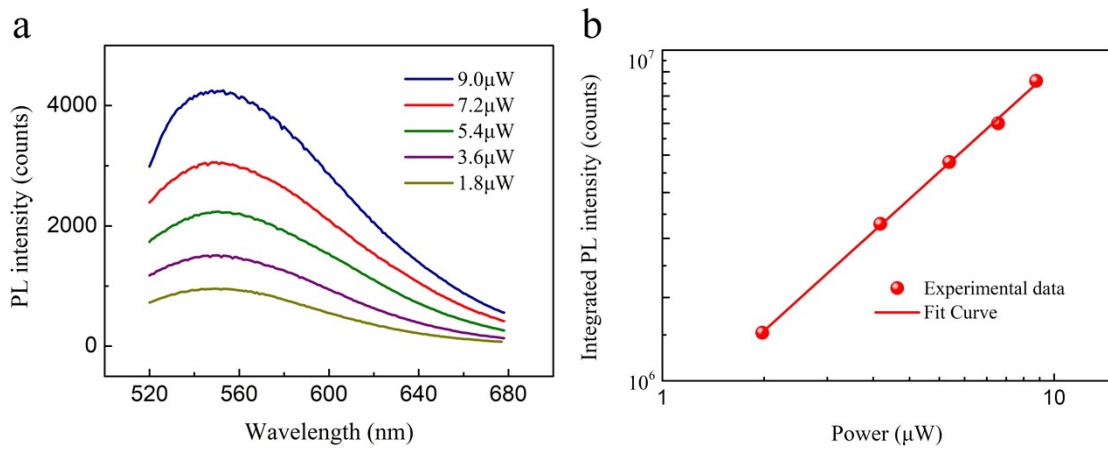| Sample τ (ns)	Sample1	Sample 2	Sample 3	Sample 4
τ_{f580}	1.52	1.75	1.94	2.32
τ_{s580}	6.98	7.74	8.57	9.15

Fig. S8. Power dependence of the emissions at long wavelength. (a) Measured PL spectra with various excitation power. b, Log-log plots of integrated PL intensity as a function of laser power. From the fitting curves, the integrated PL grows sub-linearly with the excitation power, with a slope of $\alpha = 0.11$.
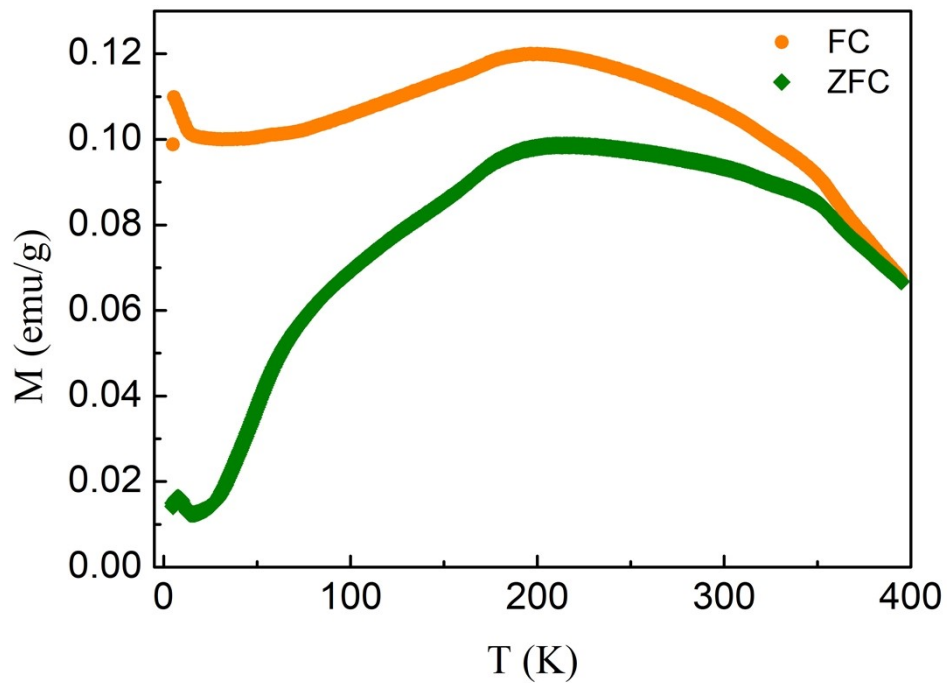
Fig. S9. Temperature dependence of the magnetic susceptibility measured at 200 Oe external magnetic-field cooling (FC) and zero magnetic-field cooling (ZFC).
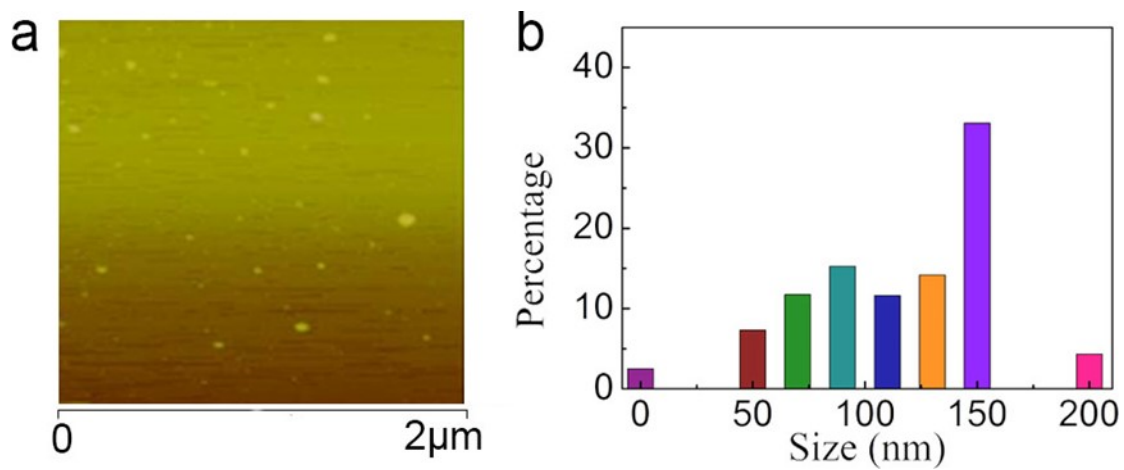
Fig. S10. AFM (a) and Size distribution (b) of the controllably oxidized BP nanosheets with

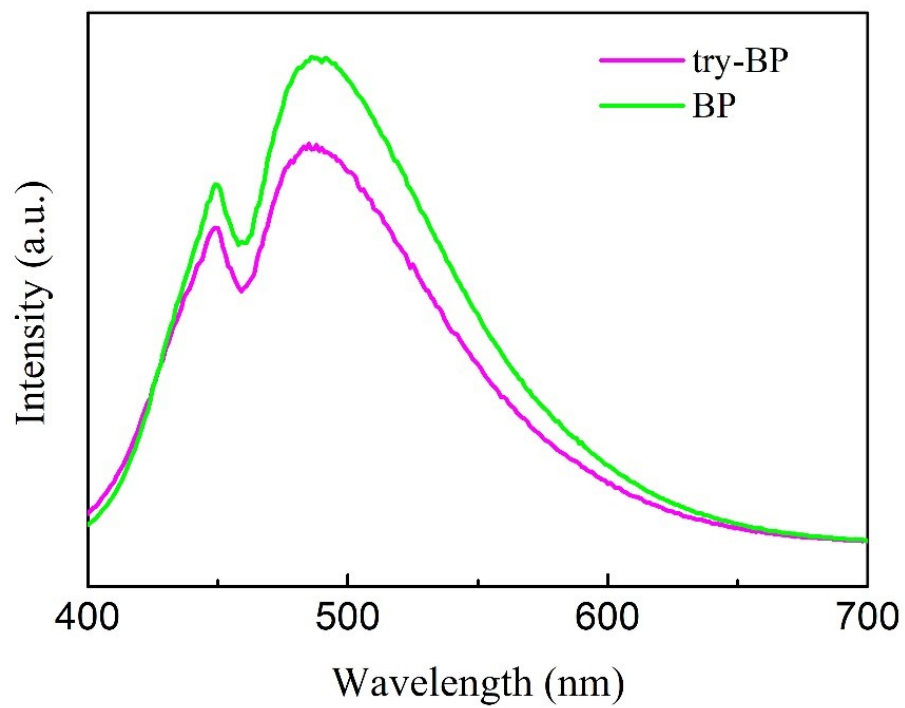tryptophan modification (total number = 300).

Fig. S11. PL spectra of the controllably oxidized BP nanosheets before and after tryptophan

modification with the excitation wavelength of 380 nm.